



## Flower-like boehmite nanopowders obtained at low temperature from Bayer liquor

Marija Milanović<sup>1,\*</sup>, Zoran Obrenović<sup>2,3</sup>, Ivan Stijepović<sup>1</sup>, Ljubica M. Nikolić<sup>1</sup>

<sup>1</sup>University of Novi Sad, Faculty of Technology Novi Sad, Department of Materials Engineering, Novi Sad, Serbia

<sup>2</sup>University of East Sarajevo, Faculty of Technology, Zvornik, Republic of Srpska, Bosnia and Herzegovina

<sup>3</sup>Alumina Ltd., Zvornik, Republic of Srpska, Bosnia and Herzegovina

Received 3 February 2020; Received in revised form 14 April 2020; Accepted 26 April 2020

### Abstract

Boehmite nanocrystalline powders were obtained by neutralization of Bayer liquor at 70 °C with addition of glucose. Temperature of the neutralization induced formation of the flower-like morphology of the nanopowders. XRD and FTIR results confirmed that the single phase boehmite is formed without any other impurities. Calcination at 500 °C led to the formation of transition  $\gamma$ -alumina with the retention of the flower-like morphology. Both as-synthesised and calcined powders possessed high specific surface area with mesopores between 3–6 nm in diameter. Relatively low temperature of neutralization as well as the use of low cost and ecologically friendly glucose as a surfactant are very promising for the possible application in the industrial production of alumina nanopowders.

**Keywords:** boehmite, chemical preparation, porosity, flower-like powders

### I. Introduction

Boehmite is an aluminium oxyhydroxide ( $\gamma$ -AlOOH), which is used as a precursor for many aluminium oxide materials especially for the preparation of ceramic catalysts, membranes, coatings, adsorbents, photoluminescent materials [1,2]. Due to its biocompatibility, another important area of interest is the use of boehmite as an orthopaedic and dental material or drug carrier [3–5]. Hydrothermal synthesis is one of the usual methods for obtaining the boehmite particles [1,6,7]. However, due to the nature of the hydrothermal method, the scale-up of the production is very hard to achieve.

Usually surfactants are added during the synthesis in order to obtain different morphology and shape of the boehmite or change pore size and specific surface area [1,7–10]. In our previous work [11] we have showed that glucose as a non-ionic surfactant enables synthesis of the pure boehmite nanopowder with ink-bottle shaped pores at room temperature.

In this work we report on the possibility to ob-

tain crystalline boehmite at relatively low temperature (70 °C) under ambient conditions where the formation of gibbsite or bayerite is avoided. We have synthesized pure nanocrystalline boehmite powders with high surface area and flower-like morphology using a low-cost and non-toxic glucose, starting from industrial Bayer liquor. The influence of concentration of the starting sodium aluminate solution and concentration of glucose on textural properties of the obtained boehmite powders was studied.

### II. Experimental

Nanocrystalline boehmite powders were synthesized starting from sodium aluminate solution prepared from Bayer liquor. The sodium aluminate solution was provided by the company Alumina Ltd., Zvornik, Bosnia and Herzegovina. Glucose was added in the starting solution as a surfactant. The neutralization of the starting solution having pH = 11.9 was performed with the use of 1 M sulphuric acid until pH decreased down to 9.5. During neutralization procedure, solution was stirred at 70 °C for 60 min. The obtained white precipitate was separated by vacuum filtration, washed with distilled

\*Corresponding author: tel: +381 21 485 3758,  
e-mail: [majam@uns.ac.rs](mailto:majam@uns.ac.rs)

**Table 1. Sample notations and parameters during synthesis**

Sample notation	Al <sub>2</sub> O <sub>3</sub> /Glucose [mol/mol]	Concentration of sodium aluminate solution
AG25-10	1 : 10	25 g/l Na <sub>2</sub> O <sub>k</sub>
AG25-20	1 : 20	25 g/l Na <sub>2</sub> O <sub>k</sub>
AG25-50	1 : 50	25 g/l Na <sub>2</sub> O <sub>k</sub>
AG50-10	1 : 10	50 g/l Na <sub>2</sub> O <sub>k</sub>

water to remove residual ions and dried at 110 °C for 3 h. The as-synthesized powders were heated in air at 500 °C for 3 h with a heating rate of 5 °C/min. In order to investigate the influence of the process parameters on the structure and morphology of the obtained powders, the starting sodium aluminate concentration and concentration of glucose were modified. In this way, we have obtained samples presented in Table 1. The calcined samples were noted in the same way as the as-synthesized samples with the addition of the letter “c”.

The crystallinity and the phase composition of the obtained samples were determined by X-ray diffraction (XRD) using Rigaku MiniFlex 600 diffractometer (CuK $\alpha$  radiation,  $\lambda = 1.5406 \text{ \AA}$ ). XRD patterns were recorded in  $2\theta$  range 10–70° with a scan rate of 0.03 °/s. The morphologies and microstructure of the samples were observed through scanning electron microscope, JEOL JSM 6460 LV and transmission electron microscope, JEOL JEM 1400 Plus, operating at 120 kV. The structural changes caused during synthesis and thermal treatment of the samples were studied by Fourier transformed infrared (FT-IR) spectroscopy performed on Nicolet-Nexus 670 spectrophotometer. Adsorption/desorption characteristics of the samples were measured by nitrogen adsorption at 77 K (Micromeritics ASAP 2010 instrument) and specific surface areas were calculated by the BET method. Pore size distributions were obtained by fitting the Barret-Joyner-Hallender (BJH) model to the desorption isotherms.

### III. Results and discussion

Figure 1a shows the XRD patterns of the as-synthesized samples. All diffraction peaks can be as-

signed to boehmite phase with an orthorhombic unit cell (JCPDS No. 21-1307). The broad peaks indicate the nanocrystalline nature of the as-synthesized samples. The addition of glucose favours crystallization of the pure boehmite phase without bayerite and gibbsite impurities. With increase in the concentration of glucose and starting aluminate solution, the crystallinity of the as-synthesized powders as well as the calcined powders increases. The XRD patterns of the calcined samples, Fig. 1b, indicate that the boehmite structure transformed to the  $\gamma$ -alumina (JCPDS No. 10-0425).

Figure 2 shows the FTIR spectra of the alumina powders before and after calcination. Bands of the as-synthesized samples (Fig. 2a) correspond to the boehmite phase according to the published literature [11,12]. Two well-resolved bands at 3410 cm<sup>-1</sup> and 1634 cm<sup>-1</sup> can be assigned to the O–H stretching and H–O–H bending modes of the adsorbed water, respectively. The band at 1073 cm<sup>-1</sup> and the shoulder at 3090 cm<sup>-1</sup> are assigned to the (Al)O–H bending and stretching vibrations of boehmite, respectively. FTIR bands at around 498, 625, and 720 cm<sup>-1</sup> correspond to the vibration modes of AlO<sub>6</sub>. Therefore, FT-IR spectroscopy was consistent with the analysis of XRD. Fig. 2b shows FTIR spectra of the  $\gamma$ -alumina samples obtained after calcination. Decrease of the intensity of the hydroxyl stretching mode (at 3450 cm<sup>-1</sup>) imply on dehydroxylation of the boehmite phase and formation of the active alumina phase. Moreover, this band is shifted to the higher wavenumbers which could be attributed to the decreased distance between layers. Two bands centred at around 800 and 600 cm<sup>-1</sup> are assigned to AlO<sub>4</sub> and AlO<sub>6</sub> coordinated aluminium ions that are typical of  $\gamma$ -alumina.

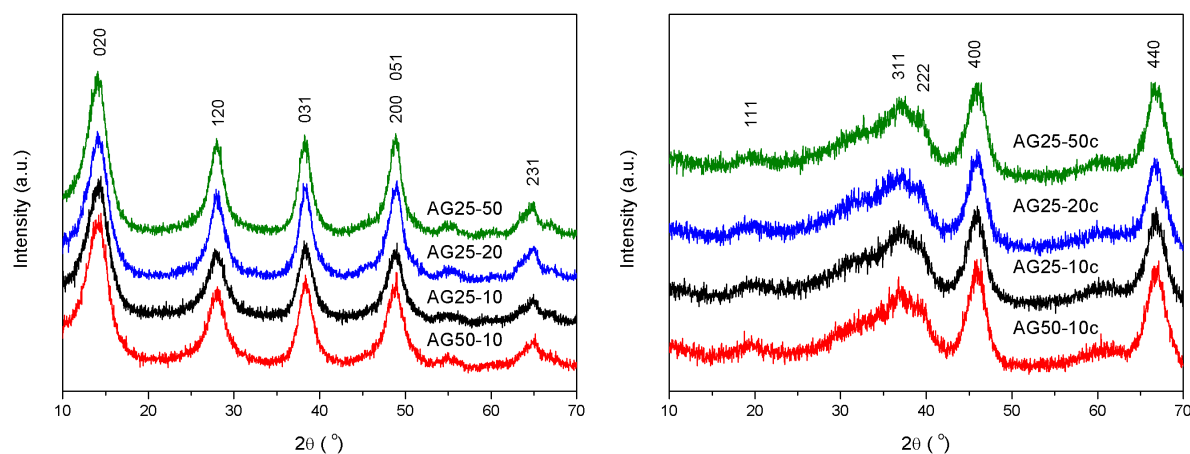


**Figure 1. XRD patterns of the alumina nanopowders: a) as-synthesized and b) calcined**

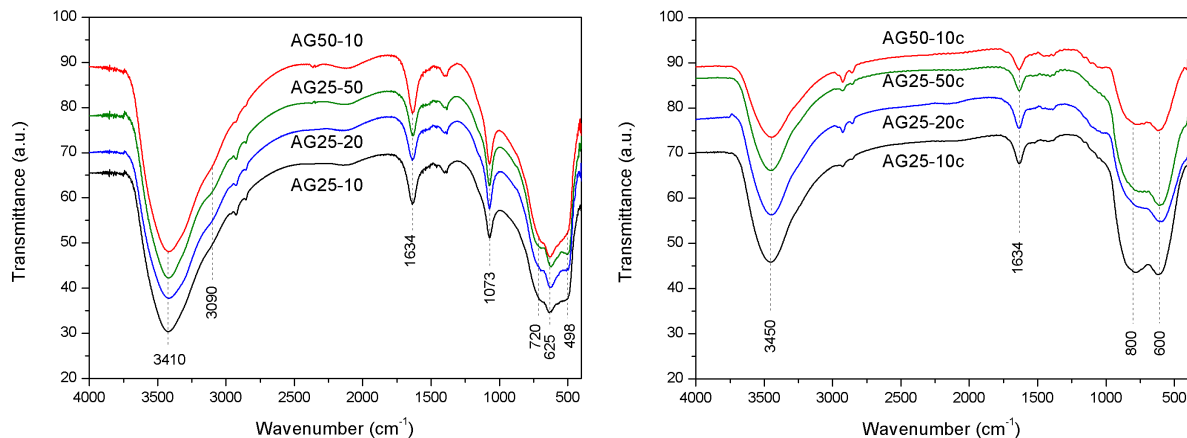


Figure 2. FTIR spectra of the alumina nanopowders: a) as-synthesized and b) calcined

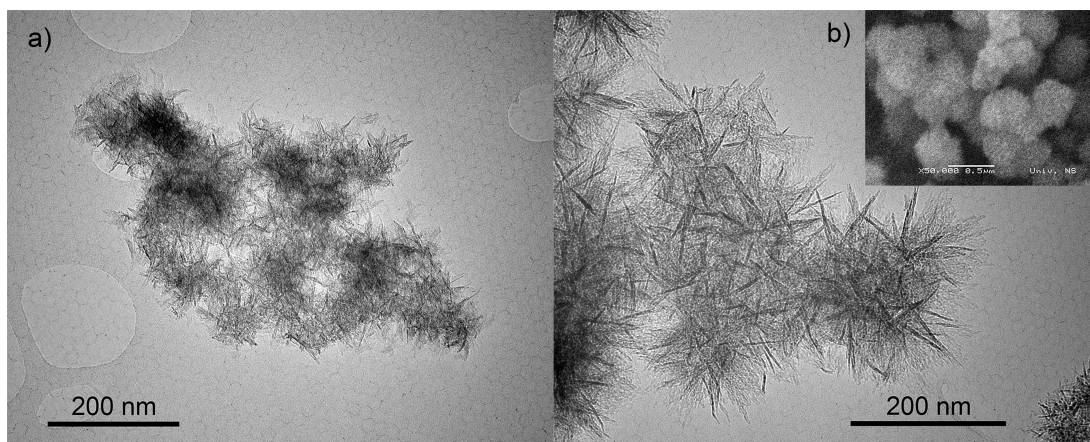


Figure 3. TEM micrographs of the alumina nanopowders: a) as-synthesized, AG25-20 and b) calcined, AG25-50c (inset: SEM image of AG25-50c)

The morphologies of the prepared alumina powders are shown in Fig. 3. The flower-like particles are obtained in all investigated samples. The surface is composed of a large number of thin lamellae. These flower-like agglomerates of the boehmite nanosheets are around 100–200 nm in size. After calcination at 500 °C, boehmite particles transform to  $\gamma$ -alumina (Fig. 1b) with retention of the morphology and with increase of the bundles size.

Figure 4 shows the pore size distributions and corresponding  $N_2$  adsorption/desorption isotherms for the as-synthesized and calcined alumina samples. The isotherms can be classified as type IV which is typical for mesoporous materials. Hysteresis loops are of H3 type, according to the IUPAC classification. Such isotherms are characteristic of plate-like nanostructures that have slit-shaped mesopores [13]. This is in accordance with TEM images that indicate the presence of

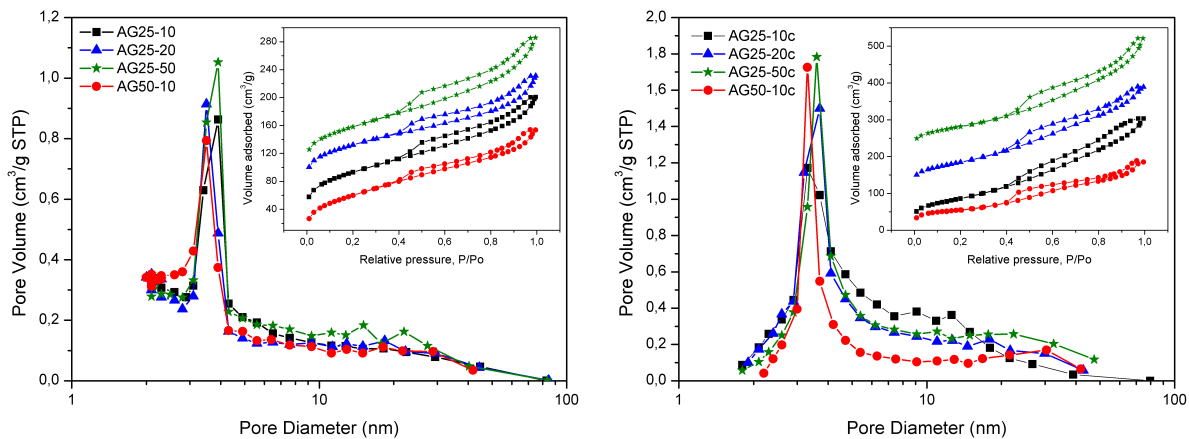
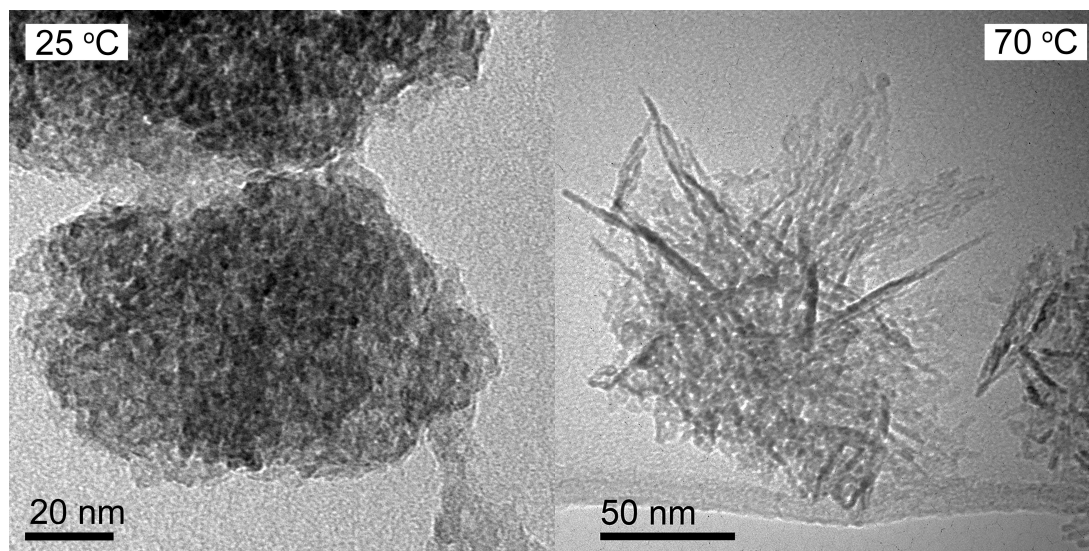


Figure 4. Nitrogen adsorption/desorption isotherms and corresponding BJH pore size distribution of the as-synthesized (a) and calcined alumina nanopowders (b)

**Table 2. Textural characteristics (specific surface area  $S_{BET}$ , total pore volume  $V_p$  and pore diameter  $D_p$ ) of as-synthesized and calcined alumina nanopowders**

Samples	As-synthesised			Calcined at 500 °C		
	$S_{BET}$ [m <sup>2</sup> /g]	$V_p$ [m <sup>3</sup> /g]	$D_p$ [nm]	$S_{BET}$ [m <sup>2</sup> /g]	$V_p$ [m <sup>3</sup> /g]	$D_p$ [nm]
AG25-10	331.5	0.291	3.5	310.5	0.441	5.7
AG25-20	293.6	0.258	3.5	307.1	0.427	5.6
AG25-50	314.6	0.308	3.9	295.3	0.456	6.2
AG50-10	320.4	0.268	3.4	194.3	0.279	5.7

**Figure 5. TEM images of the boehmite powder AG25-10 obtained at room temperature and at 70 °C**

non-rigid aggregates of the lamellar framework. The hysteresis loop in all samples closes very near to  $P/P_0 = 1$  with no obvious plateau, so that there could be some macroporosity present in the samples [14]. This is probably related to the inter-particle porosity that connects the mesoporous particles. All samples show a pore size distribution within the mesoporous range. The slit-shaped pores are about 3–6 nm wide as calculated by the Barrett-Joyner-Halenda (BJH) method. Textural characteristics presented in Table 2 indicate that the shape and size of the pores have little or no dependence on the applied treatment (i.e. concentration of glucose and sodium aluminate solution). This result is consistent with the stability of the specific surface area. The large specific surface area obtained for alumina samples is comparable with the ones in the literature [15–18] with similar flower-like spherical morphology.

It is interesting to point out that the temperature during neutralization procedure strongly influences the pore morphology. As we previously reported, during neutralization at room temperature [11] and at 70 °C (this work) we have obtained mesoporous alumina powders. However, porous structure of these powders' changes from ink-bottled to slit-shaped when the temperature is raised from 25 to 70 °C during neutralization. In addition, the morphology of the powders is changed too, Fig. 5. Hence, the glucose as a non-directing agent is an essential element for creating the mesoporosity inside the particles, but the choice of the temperature during neutralization procedure affects the shape of the

pores and morphology of the powders. A thermal activation at relatively low temperature has a drastic impact on the porosity. This could be potentially important regarding the choice of the particles for specific application, but what is more important, regarding the economic feasibility of the production process of the desired porosity within powders.

Li *et al.* [19] have prepared flower like alumina nanoparticles starting from sodium aluminate solution and using urea as structure directing agent. They suggested a three-step growth mechanism, where starting irregular particles through oriented growth form flake-like nanopetals which then assemble into the flower-like particles. The high concentration of  $\text{OH}^-$  in the system speed up the reaction and transfer rate in this Oswald ripening process. Having in mind that glucose has five hydroxyl ( $\text{OH}^-$ ) groups and that at 70 °C the rate of the ripening process would increase, the suggested growth mechanism could explain the change in the morphology of our samples with the increase of the temperature. However, more detailed study should be done and one more parameter needs to be accounted for (the reaction time), in order to define the exact growth mechanism.

The presented flower-like architectures and high BET surface areas suggest potential application in water treatment. Heavy metal ions, such as Pb, Hg, Cd, Cr, Mn etc., are highly toxic water pollutants, harmful for human health, so their efficient removal from water is of great importance. Preliminary results showed that the alumina particles prepared in a suggested way exhibited

the great performance towards chromium removal from the water.

#### IV. Conclusions

In this work flower-like boehmite nanoparticles were obtained at low temperature from Bayer liquor. The glucose was used as promoter of the boehmite powder formation with narrow particle size and high surface area. The morphology and textural characteristics of alumina powders are maintained after thermal treatment at 500 °C. The results have showed that it is possible to prepare a high-quality powder in a wide range of used concentrations of glucose and industrial Bayer liquor. However, it is important to highlight that tuning the textural properties of the alumina nanopowders is possible by changing the temperature from RT to 70 °C during neutralization procedure. Hence, the ease and low cost of the presented procedure show great promise for industrial-scale production of boehmite and transition alumina nanopowders.

**Acknowledgement:** The authors acknowledge the financial support from the Serbian Ministry of Education, Science and Technological Development, Project No. 451-03-68/2020-14/200134. We thank Dr. Sanja Panić for nitrogen adsorption measurements and Dr. Vladimir Pavlović for TEM measurements.

#### References

1. X. Wu, B. Zhang, Z. Hu, "Large-scale and additive-free hydrothermal synthesis of lamellar morphology boehmite", *Powder Technol.*, **239** (2013) 155–161.
2. E. Kiss, G. Boskovic, "Impeded solid state reactions and transformations in ceramic catalysts supports and catalysts", *Process. Appl. Ceram.*, **6** (2012) 173–182.
3. T.J. Webster, E.L. Hellenmeyer, R.L. Price, "Increased osteoblast functions on theta+delta nanofiber alumina", *Bio-materials*, **26** (2005) 953–960.
4. G. Mohammadnezhad, M. Dinari, A. Nabiyan, "High surface area nano-boehmite as effective nano-filler for preparation of boehmite-polyamide-6 nanocomposites", *Adv. Polym. Technol.*, **37** (2018) 1221–1228.
5. Y.V. Solovov, A.Y. Prilepskii, E.F. Krivoshapkina, A.F. Fakharo, E.A. Bryushkova, P.A. Kalikina, E.I. Koshel, V.V. Vinogradov, "Sol-gel derived boehmite nanostructures is a versatile nanoplatform for biomedical applications", *Sci. Rep.*, **9** (2019) 1176.
6. S. Zanganeh, A. Kajbafvala, N. Zanganeh, M.S. Mohajerani, A. Lak, M.R. Bayati, H.R. Zargar, S.K. Sadrnezhad, "Self-assembly of boehmite nanopetals to form 3D high surface area nanoarchitectures", *Appl. Phys. A*, **99** (2010) 317–321.
7. Z. Tang, J. Liang, X. Li, J. Li, H. Guo, Y. Liu, C. Liu, "Synthesis of flower-like boehmite ( $\gamma$ -AlOOH) via a one-step ionic liquid-assisted hydrothermal route", *J. Solid State Chem.*, **202** (2013) 305–314.
8. J. Zhou, L. Wang, Z. Zhang, J. Yu, "Facile synthesis of alumina hollow microspheres via trisodium citrate-mediated hydrothermal process and their adsorption performances for p-nitrophenol from aqueous solutions", *J. Colloid Interf. Sci.*, **394** (2013) 509–514.
9. W. Lueangchaichaweng, B. Singh, D. Mandelli, W.A. Carvalho, S. Fiorilli, P.P. Pescarmona, "High surface area, nanostructured boehmite and alumina catalysts: Synthesis and application in the sustainable epoxidation of alkenes", *Appl. Catal. A*, **571** (2019) 180–187.
10. Z. Ecsedi, I. Lazău, C. Păcurariu, "Synthesis of mesoporous alumina using polyvinyl alcohol template as porosity control additive", *Process. Appl. Ceram.*, **1** (2007) 5–9.
11. M. Milanović, Z. Obrenović, I. Stijepović, Lj.M. Nikolić, "Nanocrystalline boehmite obtained at room temperature", *Ceram. Int.*, **44** (2018) 12917–12920.
12. T.C. Alex, R. Kumar, S.K. Roy, S.P. Mehrotra, "Leaching behaviour of high surface area synthetic boehmite in NaOH solution", *Hydrometallurgy*, **137** (2013) 23–32.
13. G. Mohammadnezhad, O. Akintola, W. Plass, F. Steiniger, M. Westermann, "A facile, green and efficient surfactant-free method for synthesis of aluminum nanooxides with an extraordinary high surface area", *Dalt. Trans.*, **45** (2016) 6329–6333.
14. F.M. Segal, M.F. Correa, R. Bacani, B. Castanheira, M.J. Politi, S. Brochsztain, E.R. Triboni, "A novel synthesis route of mesoporous  $\gamma$ -alumina from polyoxohydroxide aluminum", *Mater. Res.*, **21** (2018) e20170674.
15. A.S. Lozhkomoev, E.A. Glazkova, O.V. Bakina, M.I. Lerner, I. Gotman, E.Y. Gutmanas, S.O. Kazantsev, S.G. Psakhie, "Synthesis of core-shell AlOOH hollow nanospheres by reacting Al nanoparticles with water", *Nanotechnology*, **27** (2016) 205603.
16. B. Fang, Z. Bao, L. Lu, L. Zhao, H. Wang, "Preparation of a hierarchical flower-like  $\gamma$ -Al<sub>2</sub>O<sub>3</sub>@C composite exhibiting enhanced adsorption performance for congo red by high temperature transformation of  $\gamma$ -AlOOH@C precursors", *RSC Adv.*, **6** (2015) 61–64.
17. C. Wang, S. Huang, L. Wang, Z. Deng, J. Jin, J. Liu, L. Chen, X. Zheng, Y. Li, B.L. Su, "Gas leaching as a path to build hierarchical core-corona porous alumina nanostructures with extraordinary pollutant treatment capacity", *RSC Adv.*, **3** (2013) 1699–1702.
18. Y. Cai, H. Huang, L. Wang, X. Zhang, Y. Yuan, R. Li, H. Wan, G. Guan, "Facile synthesis of pure phase  $\gamma$ -AlOOH and  $\gamma$ -Al<sub>2</sub>O<sub>3</sub> nanofibers in a recoverable ionic liquid via a low temperature route", *RSC Adv.*, **5** (2015) 104884–104890.
19. Y. Li, Z. Wu, F. Zhao, X. Gong, "Facile template-free fabrication of novel flower-like  $\gamma$ -Al<sub>2</sub>O<sub>3</sub> nanostructures and their enhanced Pb(II) removal application in water", *Cryst. Eng. Commun.*, **18** [21] (2016) 3850–3855.